Nuclear Physics A515 (1990) 409-432
North-Holland

SUPERFLUIDITY IN NEUTRON MATTER AND NUCLEAR MATTER WITH REALISTIC INTERACTIONS

M. BALDO[1], J. CUGNON[2], A. LEJEUNE[2] and U. LOMBARDO[1]

[1] *Dipartimento di Fisica, Univ. di Catania and INFN sezione di Catania, Corso Italia 57, I-95129 Catania, Italy*

[2] *Université de Liège, Physique Nucléaire Théorique, Institut de Physique au Sart Tilman, Bâtiment B.5, B-4000 Liege 1, Belgium*

Received 22 February 1990
(Revised 19 April 1990)

Abstract: The $^1S_0$ superfluidity of neutron matter and nuclear matter is studied by solving the gap equation exactly for two realistic nuclear potentials, namely the Paris and the Argonne v_{14} potential. For neutron matter, the predicted domain of superfluidity is very close to previous results, whereas differences appear in the predicted value of the maximum gap. The results are, however, very close to each other for the two potentials mentioned above. The role of the large momentum component is underlined and the accuracy of several approximations is discussed. The temperature dependence is exhibited. For nuclear matter, the superfluidity disappears at smaller density. The gap is rather small for equilibrium density. The condensation energy estimated through a local-density approximation is dominated by the surface contribution. The definition of the pairing interaction is discussed and an illustrative calculation for an effective interaction is presented.

1. Introduction

It was already pointed out a long time ago [1]), that the spectrum of even-even nuclei presents an "energy gap", that could be described in a manner similar to the one invented by Bardeen, Cooper and Schrieffer [2]) (BCS) for superconductivity. Soon after, Cooper, Mills and Sessler [3]) showed that the BCS method can be applied to infinite systems of strongly interacting fermions. It was also realized that nuclear matter and, even better, neutron matter could in fact exist in a superfluid state for a wide class of nucleon-nucleon potentials [4]) in some density range. Nuclear matter superfluidity is perhaps a somewhat academic problem, since ordinary uniform nuclear matter can show a lot of various instabilities [5]) which are expected to mask superfluidity in a broad range of densities (see our remark below, however). Neutron matter superfluidity is expected to lead to interesting macroscopic phenomena in neutron stars, as was first pointed out by Migdal [6]) as early as thirty years ago. According to modern views [7]), nucleonic superfluidity enters in three aspects of neutron star physics. First, at the surface of the star, a neutron gas, pervading a lattice of neutron-rich nuclei and a sea of relativistic electrons, exists at densities allowing strong pairing of neutrons in the $^1S_0$ state. More inside the star, nuclei dissolve and the fluid is a mixture of neutrons, protons, electrons and muons. The density is such that $^1S_0$ pairing of protons is foreseeable. The inner part of the star

contains high-density neutron matter, which is presumably the seat of anisotropic $^3P_2{}^3F_2$ pairing.

Superfluid properties have been studied for a long time [8-20]), mainly with phenomenological forces and using simplifying approximations, like the introduction of a cut-off in solving the gap equation encountered in BCS theory. However, realistic interactions have been used in most recent works [17-21]). Furthermore, several investigations have been made to cast BCS theory in a sophisticated many-body theoretical scheme. Yet, it is remarkable that all calculations yield qualitatively similar results for the $^1S_0$ pairing, namely that neutron matter is superfluid for densities with a Fermi momentum k_F less than ~ 1.3–$1.5\ \mathrm{fm}^{-1}$. However, the value of maximum gap at the Fermi surface as well as the condensation energy vary quite importantly from one calculation to another, even if one restricts to so-called realistic interactions. In particular, the effect of the polarization interaction seems to be very important [21]) (see discussion below, however).

Recently, the interest in superfluid properties of neutron matter as well as nuclear matter has been revived by several works. In ref. [21]), the authors study neutron matter superfluidity in the frame of the so-called correlated basis formalism. In ref. [22]), thermodynamics of nuclear matter is studied with the use of Skyrme forces. In ref. [23]), the gap equation is solved without limiting assumptions for the effective Gogny force [24]). Let us also mention the interesting work of ref. [25]), which attempts to derive a formalism for describing superfluidity without violating particle-number conservation, like it is the case in BCS theory.

Our purpose is to study superfluidity, both in neutron and nuclear matter using the Paris potential [26]). The latter, one of the most modern nucleon–nucleon potentials, has been shown to describe correctly the nucleon–nucleon data and to yield reasonable results for nuclear-matter binding energy (with the help of three-body forces [27])) as well as for single-particle properties within nuclear matter [28]). It is thus natural to look whether or not this interaction gives good results for collective properties like pairing. Theoretically, the superfluidity problem can be tackled by sophisticated many-body formalisms. However, most of them are not suited for numerical investigations and, in practice, one is reduced to use the conventional BCS theory, using more and more refined pairing interaction by adding successive corrections to the nucleon–nucleon interaction. This paper deals with the simplest problem of this program, namely the study of the $^1S_0$ pairing, using conventional BCS theory and solving exactly the gap equation, for the bare interaction mainly (see discussion in sect. 2.2 for this choice). This is not without practical interest, in view of the scattered results obtained previously within this scheme. In addition, in this first approach, we want also to concentrate on some technical points concerning the gap equation. Furthermore, as it turns out that the Paris potential exhibits special features which make the solution of the gap equation a delicate task (see below), we also used another realistic interaction (the v_{14} Argonne potential [29])) for the sake of comparison and of supplementary check.

Our paper is organized as follows. Sect. 2 is a reminder of the formalism leading to the gap equation and elaborates on the effective interaction. In sect. 3, we show our results for the Paris and Argonne potentials, concerning superfluidity properties of neutron and nuclear matter. In sect. 4, we discuss some of the properties of the gap equation. Sect. 5 contains an analysis of our results and a discussion of their implications. We compare with related works in sect. 6. Finally, sect. 7 contains our conclusion.

2. Formalism

2.1. REMINDER OF BCS THEORY

The description of the original BCS theory can be found in standard textbooks [30-32]). We just here recall the main aspects and point out the difficulties when dealing with strongly interacting fermions. The basic premise of the BCS approach is the assumption that in first approximation, the system can be described by a wave function of an uncorrelated state $|\phi_0\rangle$, a Slater determinant of plane waves for occupied single-particle states of momentum $\boldsymbol{k}$, with $|\boldsymbol{k}|$ less than the Fermi momentum k_F and of energy $e(k)$, possibly including an average field contribution. According to BCS theory, superfluidity appears when correlations, leading to Cooper pairs (with vanishing spin and momentum), give rise to an extra binding energy which overcompensates the increase of kinetic energy due to the accompanying depopulation of the Fermi sea. In other words, one looks for a correlated state of the form

$$|\psi\rangle = \prod_k (u_k + v_k a^\dagger_{k\uparrow} a^\dagger_{-k\downarrow})|\phi_0\rangle\,, \tag{2.1}$$

giving an expectation value of the operator $H - \mu N - TS$ smaller than the one given by $|\phi_0\rangle$ (the quantity μ is the chemical potential and the free Fermi gas entropy S is usually introduced at nonzero temperature T). This happens when the gap equation (here readily particularized to isotropic pairing)

$$\Delta_k = -\int \frac{\mathrm{d}^3\boldsymbol{k}}{(2\pi)^3}\, V_{k,k'} \frac{\Delta_{k'}}{2E_{k'}} \tanh\left(\tfrac{1}{2}\beta E_{k'}\right) \tag{2.2}$$

has a non-trivial solution for the gap function Δ_k. In this equation, β is the inverse temperature, E_k is the quasi-particle energy

$$E_k = [(e(k)-\mu)^2 + \Delta_k^2]^{1/2}\,, \tag{2.3}$$

and $V_{k,k'}$ is the pairing matrix element

$$V_{k,k'} = \langle \boldsymbol{k}\uparrow -\boldsymbol{k}\downarrow | V(^1\mathrm{S}_0) | \boldsymbol{k}'\uparrow -\boldsymbol{k}'\downarrow\rangle\,, \tag{2.4}$$

where $V\,(^1\mathrm{S}_0)$ is the basic interaction in the $^1\mathrm{S}_0$ channel. In the last equation, there is no dependence upon the directions of the $\boldsymbol{k}$ and $\boldsymbol{k}'$ vectors.

2.2. THE PAIRING INTERACTION

We will not enter now into a discussion of the pairing interaction (we postpone it to sect. 7). This point is not very often discussed in the many works calculating the pairing properties. Furthermore, the proper definition of the pairing interaction does not appear clearly from the variational derivation of the gap equation. The Green function formalism [30,31]) gives, however, an unambiguous answer to this problem, namely that the pairing interaction should be taken as the sum of all irreducible graphs in the two-particle channel. In the lowest order, it reduces to the *bare* interaction. The next order involves the so-called polarization interaction. Its calculation is not obvious and previous calculations yield contradictory predictions for its effect. Therefore, we restrict ourselves in this paper to the lowest order, leaving the investigation of the polarization graph for a forthcoming publication. Even in lowest order, the calculations with realistic interactions are rather scarce.

In spite of the indications provided by the Green function approach, some authors (see e.g. refs. [13,17,18])) introduced a "medium-renormalized" interaction, as the Brueckner g-matrix or a more or less equivalent interaction in the so-called variational and hypernetted-chain approaches. In view of this situation and for the sake of illustration, we also solve the gap equation for the g-matrix in some particular cases. Of course, medium renormalization should be accounted for in the single-particle energies $e(k)$. Below, in every case, they are calculated in the Brueckner–Hartree–Fock approximation.

2.3. HIGH-MOMENTUM COMPONENTS

The gap equation is usually solved by iteration (see below), where an estimate of the function Δ_k at some step is introduced in the denominator of the kernel of the integral equation (2.2) to get another (better) estimate of Δ_k. The difficulty arises from the fact that the kernel is very sensitive to a modification of $\Delta_{k'}$ for k' close to k_F, whereas it is much less for large k'. In other words, eq. (2.2) is almost linear in the high-momentum regime, whereas it is highly nonlinear in the small-momentum range ($k \approx k_F$). Therefore, it is advisable, as advocated by Anderson and Morel [33]), to more or less disconnect the two momentum regimes. This can be done by introducing a reduced interaction $\tilde{V}$

$$\tilde{V}_{k,k'} = V_{k,k'} - \int_{k''>k_c} \frac{d^3k''}{(2\pi)^3} V_{k,k''} \frac{1}{2E_{k''}} \tilde{V}_{k'',k'}, \tag{2.5}$$

in which case the gap equation reduces to (for $T=0$)

$$\Delta_k = -\int_{k'<k_c} \frac{d^3k'}{(2\pi)^3} \frac{\tilde{V}_{k,k'}}{2E_{k'}} \Delta_{k'}, \tag{2.6}$$

if it is solved self-consistently with eq. (2.5). The solution of (2.6) is exactly equal to the solution of eq. (2.2) for $k < k_c$. The interest of this formulation is that $\tilde{V}_{k,k'}$

is almost independent of the gap and that the iterative solution of eq. (2.6) is much more stable when the range of k' is limited. We checked that all our results below do not depend upon the choice of the cut-off momentum k_c. We want to stress that for the Paris potential, the integration in eq. (2.5) has to be carried out numerically up to large values of k'' ($\geqslant 50\,\mathrm{fm}^{-1}$). The v_{14} potential is easier to handle since the integral (2.5) converges much more rapidly (see discussion in sect. 4).

2.4. FORMULA FOR $^1S_0$ PAIRING AND SEPARABLE INTERACTION

Let the interaction in the $^1S_0$ channel be separable of rank N

$$V_{k,k'} = \sum_{i,j=1}^{N} \lambda_{ij} g_i(k) g_j(k') , \tag{2.7}$$

where the g_i functions are some form factors. Then it is easy to show that $\tilde{V}_{k,k'}$ can be written as

$$\tilde{V}_{k,k'} = \sum_{i,j=1}^{N} \Lambda_{ij} g_i(k) g_j(k') , \tag{2.8}$$

with

$$\Lambda_{ij} = \{[\lambda^{-1} - \Gamma]^{-1}\}_{ij} , \tag{2.9}$$

where λ is the matrix of elements λ_{ij} and the matrix Γ is given by

$$\Gamma_{ij} = -4\pi \int_{k_c}^{\infty} \mathrm{d}k'' \frac{k''^2}{(2\pi)^3} \frac{g_i(k'') g_j(k'')}{2E(k'')} . \tag{2.10}$$

The solution of eq. (2.6) has the form

$$\Delta_k = \sum_{i=1}^{N} c_i g_i(k) \tag{2.11}$$

and eq. (2.6) itself is now equivalent to:

$$c_i = -\sum_{i=1}^{N} B_{ij} c_j , \tag{2.12}$$

with

$$B_{ij} = \sum_{l} \Lambda_{il} \int_0^{k_c} \mathrm{d}k''\, k''^2 \frac{g_l(k'') g_j(k'')}{2E_{k''}} . \tag{2.13}$$

Below, eqs. (2.13), (2.8), (2.9) together with eq. (2.6) have been solved self-consistently within an iterative procedure. The starting point was taken as the constant-Δ approximation, i.e. the value which, introduced in the matrix $\boldsymbol{B}$ (eq. (2.12)), cancels the determinant of the matrix $(\mathbf{1} - \boldsymbol{B})$.

3. Numerical results for $^1S_0$ pairing

3.1. NEUTRON MATTER

3.1.1. Paris potential. We first solved the gap equation for the separable version [32]) of the Paris potential [26]), using so the bare potential as the pairing interaction. The most important result is contained in fig. 1, which shows the gap $\Delta_F (= \Delta_k$ for $k = k_F)$ at the Fermi level as a function of the Fermi momentum. It shows that superfluidity disappears for $k_F \approx 1.4\,\mathrm{fm}^{-1}$, which corresponds to a density close to $1.5 \times 10^{14}\,\mathrm{gr\,cm}^{-3}$. The maximum value of the gap occurs at $k_F \approx 0.85\,\mathrm{fm}^{-1}$ and amounts to $\Delta_F = 2.76$ MeV.

The shape of the gap function Δ_k is given in fig. 2 for a particular value of the Fermi momentum, but is typically the same in the whole density range. It is worth to notice that the gap function is rather rapidly varying close to the Fermi momentum. Furthermore, it is negative in a wide momentum range, between ~2 and ~6 fm^{-1}, and keeps oscillating farther out. We anticipate on sect. 4 and say that one can assess the rather slow decay of the gap function when k increases to the (off-diagonal) high-momentum behaviour of the Paris potential. This rather wild variation of the gap function Δ_k is not very apparent in the pairing function $D(k)$

$$D(k) = \langle a_k^\dagger a_k^\dagger \rangle = 2u_k v_k = \frac{\Delta_k}{2E_k}, \tag{3.1}$$

which is very well peaked around the Fermi momentum, as shown in fig. 3. Note that the function $D(k)$ is nevertheless asymmetric as a consequence of the variation of the gap function Δ_k with k. The value of a closely related quantity, namely the condensation energy per nucleon is given in table 1 for several densities. This quantity has a minimum for $k_F \approx 0.6\,\mathrm{fm}^{-1}$.

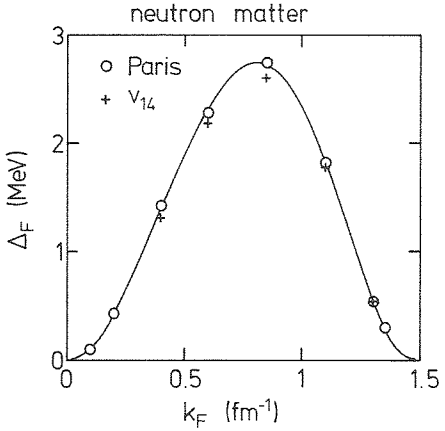

Fig. 1. Value of the gap at the Fermi surface Δ_F of neutron matter as a function of the Fermi momentum, for the Paris potential (open dots) and for the Argonne v_{14} potential (crosses).

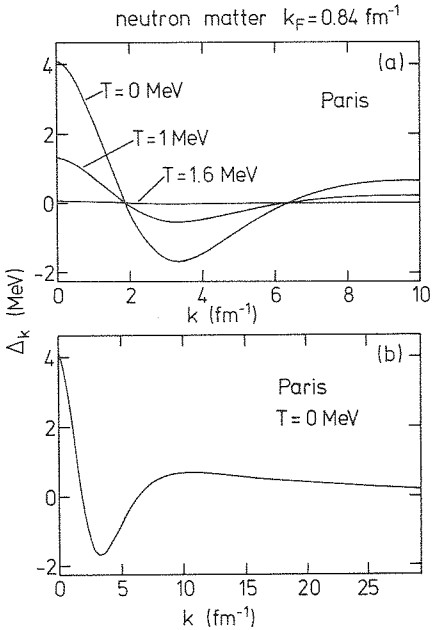

Fig. 2. Gap function Δ_k calculated for neutron matter with a Fermi momentum $k_F = 0.84\,\mathrm{fm}^{-1}$, for various temperatures (a), and at $T = 0$ for enlarged momentum scale (b).

The variation of the gap parameter at the Fermi momentum k_F as a function of the temperature T is given in fig. 4. In this calculation, the single-particle spectrum $e(k)$ has been "frozen", i.e. kept fixed independently of the temperature, which is an accurate approximation according to refs. [35,36]). The critical temperature T_c, i.e. the temperature at which the superfluid phase is no longer energetically favoured, is displayed in fig. 5 as a function of the density. It reaches a maximum of ~ 1.8 MeV for the same density as the gap Δ_F at zero temperature is maximum.

We now turn to the results obtained when using the pairing interaction as given by the g-matrix. For obvious practical reasons it is impossible to construct the corresponding reduced interaction (2.6), which in the case of the Paris potential requires the detailed knowledge of the g-matrix element $\langle \boldsymbol{k}|g|\boldsymbol{k}'\rangle$ for very large $|\boldsymbol{k}'|$ (up to $\sim 40\,\mathrm{fm}^{-1}$). We nevertheless made a calculation assuming that the relationship between the pairing interaction itself and the reduced interaction in the restricted range ($k \leqslant k_c$) is the same for the g-matrix as for the bare interaction. More precisely, we adopt the following reasonable approximation

$$\tilde{g} = \alpha g\,, \tag{3.2}$$

where

$$\alpha = \frac{\mathrm{Tr}^{(r)}\,\tilde{V}}{\mathrm{Tr}^{(r)}\,V} \tag{3.3}$$

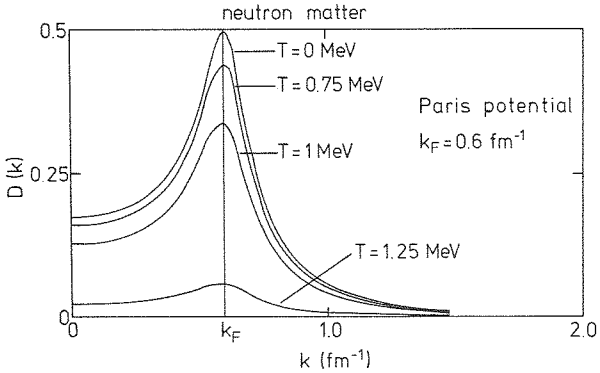

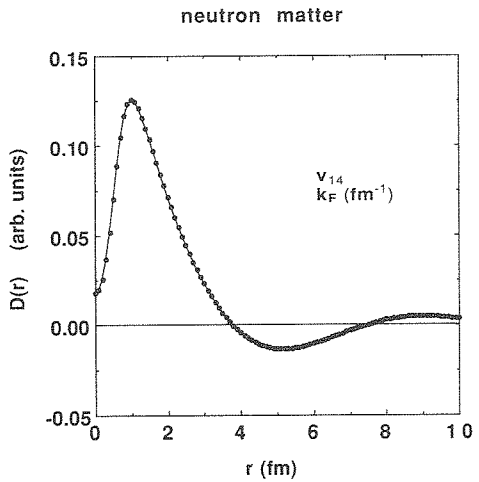

Fig. 3. (a) Pairing function $D(k)$ (eq. (3.1)) as a function of momentum k, for various temperatures T. This graph refers to neutron matter with Fermi momentum $k_F = 0.6\,\mathrm{fm}^{-1}$ and to the Paris potential. (b) Fourier transform $D(r)$ of the pairing function for v_{14} potential and $k_F = 0.84\,\mathrm{fm}^{-1}$.

TABLE 1

Comparison between the exact value of the condensation energy per nucleon in neutron matter and the value predicted by the weak coupling formula (5.8) (values in MeV)

k_F (fm^{-1})	0.1	0.2	0.4	0.6	0.84	1.1	1.3	1.35
E_C/A (exact)	−0.018	−0.121	−0.232	−0.263	−0.204	−0.077	−0.0046	−0.00044
E_C/A (eq. (5.8))	−0.016	−0.084	−0.228	−0.261	−0.188	−0.049	−0.0030	−0.00086

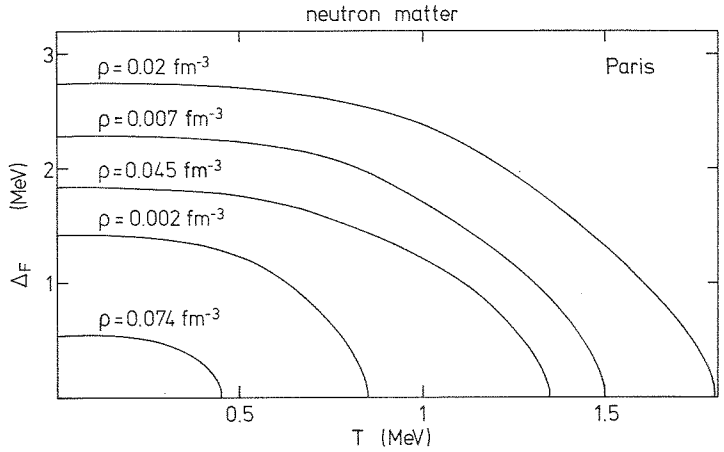

Fig. 4. Value of the gap at Fermi momentum k_F as a function of the temperature T for various (indicated) densities. This graph refers to neutron matter and to the Paris potential.

is the ratio of the traces of the reduced $\tilde{V}$ and the bare V interactions, respectively, in the restricted momentum range ($k < k_c$). Assumption (3.2) is supported by the observation that the g- and V-matrices are not so different (for $k < k_c$) from each other for the density range and the channel envisaged here. The results for the gap function at a typical density (and zero temperature) are given in fig. 6 along with the results obtained using the bare interaction. The gap at the Fermi surface is now slightly larger, although the V- and g-matrix elements are roughly similar around the Fermi surface. Once again, this is linked with the behaviour at (here relatively) large k'.

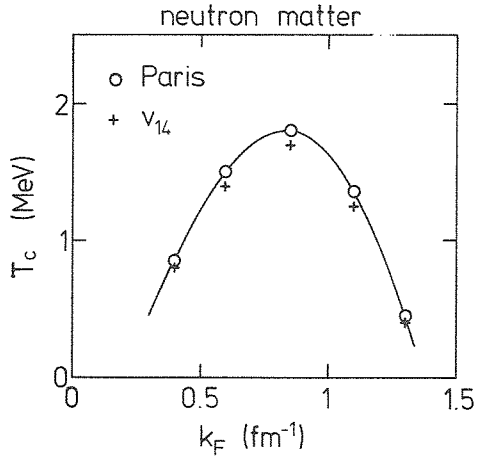

Fig. 5. Phase diagram of neutron matter for the Paris potential (open dots) and for the Argonne v_{14} potential (crosses): variation of the critical temperature T_c versus the Fermi momentum k_F.

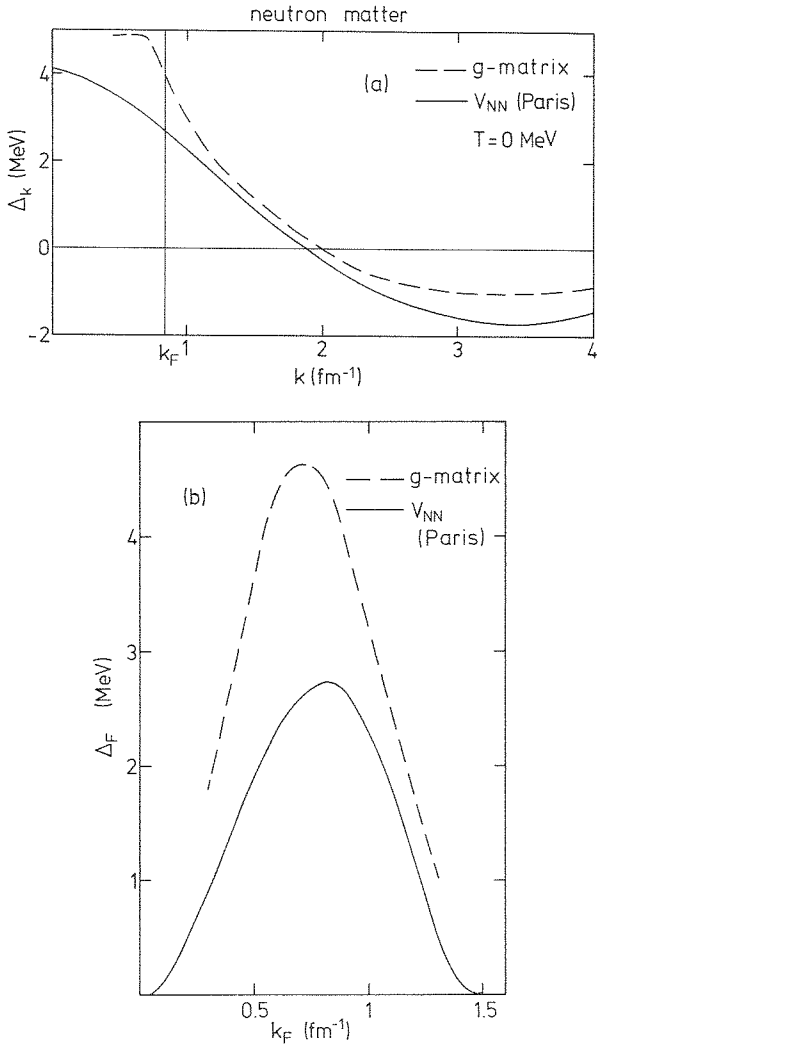

Fig. 6. Neutron matter at zero temperature. (a) Comparison of the gap function Δ_k calculated with the g-matrix (dashed curve) with the one calculated with the bare nucleon-nucleon potential (full curve). (b) Same as (a) for the gap at the Fermi momentum Δ_F as a function of the Fermi momentum k_F. See text for detail.

The variation of the zero-temperature gap Δ_F with the density is given in fig. 6b. The shape is roughly the same, but the magnitude is larger for the g-matrix.

3.1.2. The Argonne v_{14} potential. A similar study has been undertaken for this potential. More exactly, we used a separable approximation of the actual Argonne potential, constructed with the help of the so-called method of Gamow states [37]), which turns out to be more convenient than the standard Ernst, Shakin and Thaler method [38]).

The value of the gap at the Fermi surface, using the bare potential as pairing interaction, is given in fig. 1 for various densities. The domain of superfluidity does not seem to depend upon the interaction, whereas the influence of the latter is slightly more important for the value of the gap: it is smaller for the Argonne as compared to the Paris potential. The value of the gap function Δ_k is shown in fig. 7 and should be compared with fig. 2. In both cases, the gap function has roughly the same nodes, i.e. at $k \approx 2\,\mathrm{fm}^{-1}$ and at $k \sim 6\,\mathrm{fm}^{-1}$. The relative importance of the minimum (around $3.5\,\mathrm{fm}^{-1}$), compared to $\Delta_{k=0}$ is the same in both cases. However, for v_{14} the Δ_k decreases faster at large k than for the Paris potential. We will come back to this point. The temperature properties are roughly the same as for the Paris case. Therefore we do not discuss them further.

3.2. NUCLEAR MATTER

We also solve the gap equation for $^1S_0$, $T=1$ pairing in nuclear matter. If the bare interaction is used, the only difference with calculation of sect. 3.1 is the modification of the single-particle spectrum. When the latter is roughly characterized by an effective mass, nuclear matter corresponds to a smaller effective mass. It is well known that such a modification gives rise to a decrease of the gap. The results are shown in fig. 8 for the Paris potential. (Results for v_{14} are expected to be very close, see fig. 1).

We tentatively make the connection with finite nuclei, a question which has not been seriously investigated so far, by evaluating the pairing interaction energy of a nucleus E_C of mass A in a local density approximation

$$E_C = \int \frac{E_C(\rho)}{A}\,\rho(r)\,\mathrm{d}^3 r, \tag{3.4}$$

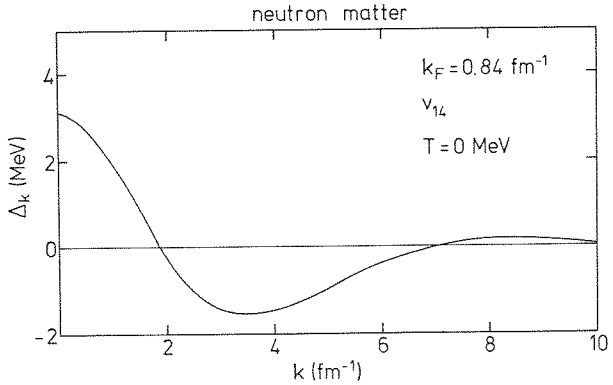

Fig. 7. Gap function calculated with the v_{14} potential for the case of cold ($T=0$) neutron matter with a Fermi momentum of $0.84\,\mathrm{fm}^{-1}$.

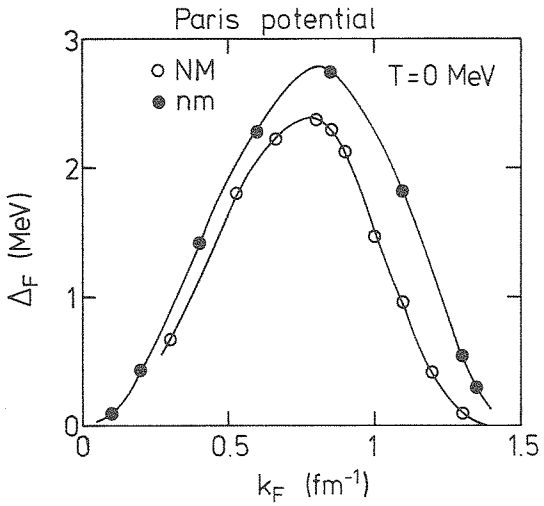

Fig. 8. Gap Δ_F at the Fermi momentum k_F as calculated with the Paris potential: comparison between nuclear matter (open dots) and neutron matter (full dots).

where the $E_C(\rho)/A$ is the condensation interaction per nucleon in nuclear matter at density ρ. This procedure may be questionable, since it is not clear that a system with a discrete single-particle spectrum can be approximated by a system with a continuous spectrum when one deals with a quantity so sensitive to the detail of the spectrum in a very narrow region. In ref. [39]), it is shown that the local-density approximation reproduces quite well the average condensation energy calculated by sophisticated Hartree-Fock-Bogoliubov calculations in finite nuclei. Our results are shown in fig. 9. One can see that the Paris potential yields good results for the condensation energy for light nuclei ($A \leqslant 60$) but underestimates it for heavy nuclei. This is of course due to the fact that Paris potential gives almost vanishing gap at $\rho \approx \rho_0$. Compared to the Gogny force [39]), this is partly compensated by a larger gap at small densities. This is why the Paris potential yields good results in light nuclei, for which the surface is proportionally more important.

4. Gap equation and off-shell behaviour

4.1. PRELIMINARIES

The $^1S_0$ gap equation writes, for $T = 0$

$$\Delta_k = -\frac{1}{2\pi^2}\int_0^\infty \mathrm{d}k'\, k'^2 \frac{v(k, k')}{2E_{k'}}\Delta_{k'}, \tag{4.1}$$

where $v(k, k')$ is the $^1S_0$ part of the pairing potential. Mathematically this integral equation is of Hammerstein type. It has a unique non-trivial solution if [40]): (i) the

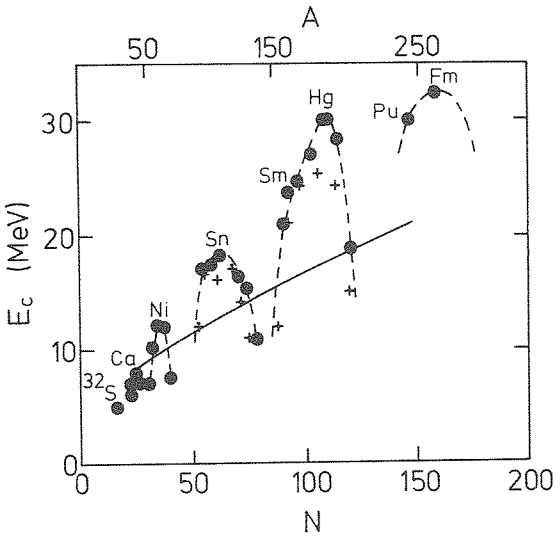

Fig. 9. Condensation energy in nuclei: Hartree-Fock-Bogoliubov (in spherical symmetry) results with the Gogny force of ref.[39]) (full dots), Hartree-Fock + BCS calculation of ref.[46]) (crosses) and our results for the Paris potential with the local-density approximation (eq. (3.4), full line).

kernel $v(k, k')$ belongs to the L_2 class; (ii) the kernel is symmetric; (iii) the kernel has all negative eigenvalues; (iv) the function

$$f(k', u) = \frac{k'^2}{2\sqrt{(e(k') - \mu))^2 + u^2}} u \tag{4.2}$$

is a non-decreasing function of u for all k', which is always satisfied. Condition (iii) corresponds physically to an attractive interaction. Note, however, that non-trivial solutions exist for potentials having some positive eigenvalues. What is needed in practice is the dominance of one or a few negative eigenvalues of $v(k, k')$. Condition (i) demands that $v(k, k')$ decreases faster than k'^{-1} for any k when $k' \to \infty$, if one restricts to integer powers of k'.

4.2. IMPORTANCE OF THE POTENTIAL AT LARGE MOMENTUM

Because of the peak observed in the function $\Delta_k/2E_k$ (see fig. 3), it is customarily stated that only the values of potential $v(k, k')$ around $k' = k_F$ are sufficient to determine the value of the gap, at least at $k = k_F$. We would like to argue that this is not true in general.

First, if $v(k, k') \sim k^{-\alpha}$ for any k' when $k \to \infty$, it is evident from eq. (4.1) that $\Delta(k) \sim k^{-\alpha}$ at large k. In the least favourable case ($\alpha = 1 + \varepsilon$, where ε is a positive infinitesimal number), integral (4.1) barely converges, which means that the large k' domain may be overwhelmingly important. In more favourable cases, this may

be less critical (see below). In any case, one can show how this comes up. We will study two cases to illustrate this point.

(i) *Separable interaction.* Let us assume that

$$v(k, k') = -\xi g(k) g(k') . \tag{4.3}$$

Let us also assume that $k_c (> k_F)$ is sufficiently large for having $|\Delta_{k'}| \ll |e(k') - \mu|$ for any $k' > k_c$. Then it is easy to show that the elimination of the large k' component amounts to use in $k < k_c$ a reduced interaction

$$\tilde{v}(k, k') = -\tilde{\xi} g(k) g(k') , \tag{4.4}$$

with

$$\tilde{\xi} = \xi \left[1 - \frac{\xi}{2\pi^2} \int_{k_c}^{\infty} \mathrm{d}k' \frac{k'^2 g^2(k')}{2|e(k') - \mu|} \right]^{-1} . \tag{4.5}$$

It is clear that high momenta can play an important role if either ξ is important or the form factor $g(k')$ extends very far in momentum.

(ii) *Effective-mass approximation.* If $e(k) = \hbar^2 k^2 / 2m^* + e(k=0)$ and if, furthermore, one assumes that one can use $\Delta_{k'} \approx \Delta_{k'=k_F} = \Delta_F$ in the expression of the quasi-particle energy, one can use the following relation

$$\frac{1}{\sqrt{(x^2-1)^2 + \alpha^2}} = \ln\left(\frac{8}{\alpha}\right) \delta(x-1) + \frac{1}{|x^2-1|} \left\{ \exp\left[(x-1) \left(\frac{\partial}{\partial x} \right)_{x=1} \right] - 1 \right\} + \mathrm{O}(\alpha) , \tag{4.6}$$

where the remaining term is at most linear in α. This relation is derived (not in this general form) in ref. [23]), where it is used to derive an approximate value of Δ_F (see also below). Eq. (4.1) can then be written (for $k = k_F$) as

$$\Delta_F \approx -\frac{1}{2\pi^2} \frac{m^*}{\hbar^2} \left[k_F \ln\left(\frac{4\hbar^2 k_F^2}{m^* \Delta_F} \right) v(k_F, k_F) \Delta_F + \int_0^{\infty} \mathrm{d}k' \frac{[k'^2 v(k_F, k') \Delta_{k'} - k_F^2 v(k_F, k_F) \Delta_F]}{|k'^2 - k_F^2|} \right] . \tag{4.7}$$

This equation clearly illustrates our point. If $v(k_F, k')$ extends very far, the value of Δ_F is less and less determined by $v(k_F, k_F)$ only (first term).

4.3. HIGH-MOMENTUM COMPONENTS OF THE PARIS AND v_{14} POTENTIALS

The matrix elements of the Paris potential (separable form) for the $^1S_0$ partial wave are given in fig. 10. The striking feature is the long tail at large k'. Analytically it behaves like k'^{-2} as the original Paris potential. A maximum occurs at $k' \approx 10\ \mathrm{fm}^{-1}$ for a particular value of k ($1\ \mathrm{fm}^{-1}$) mentioned in fig. 10c. In the original Paris potential, this maximum occurs at an even larger momentum [41]). The quantity $v(k, k')$

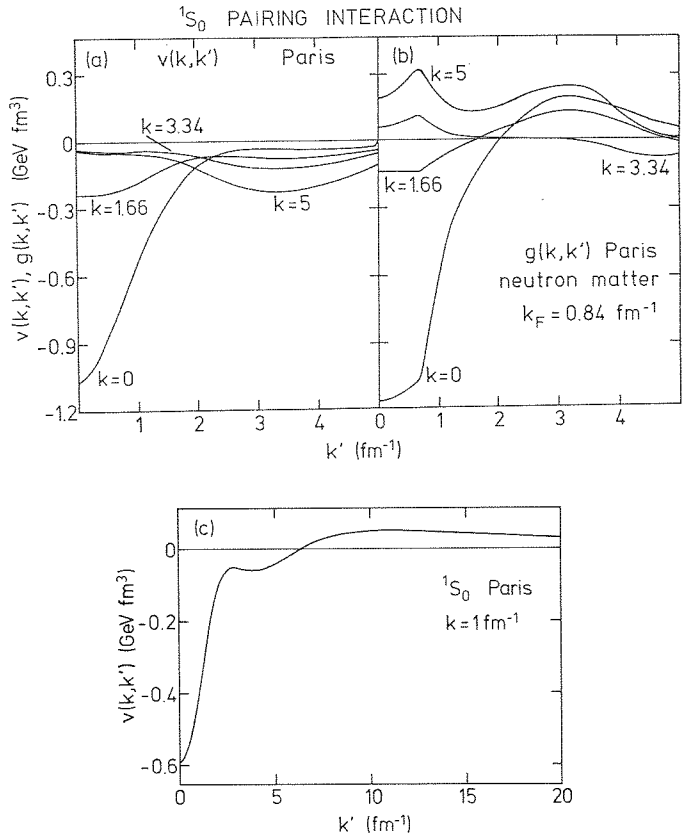

Fig. 10. Matrix elements $v(k, k')$ of the interaction in the $^1S_0$ channel as functions of momentum k' for indicated values of k (in fm^{-1}); (a) Bare nucleon–nucleon Paris interaction (finite-rank version), (b) g-matrix based on the same potential in neutron matter with momentum $k_F = 0.84\,\mathrm{fm}^{-1}$, (c) Bare interaction for an enlarged k'-momentum scale and $k = 1\,\mathrm{fm}^{-1}$.

has a zero at $k' \approx 6\,\mathrm{fm}^{-1}$ almost independently of k and nearly vanishes for $k' \approx$ 1.5–3.0 fm^{-1}, depending on the value of k. These properties can be related to the fact that the form factors entering expression (2.6) have practically the same nodes. This fact is a direct consequence of the repulsive core exhibited by any realistic interaction. The size of the core is $c \sim 0.5$ fm and shows up in every form factor in r-space. In k-space, each form factor must display a full oscillation within $k \sim \pi/c \approx$ 6 fm^{-1}. The matrix elements of the g-matrix for $k_F = 0.84\,\mathrm{fm}^{-1}$ are also shown in fig. 10 for the sake of comparison.

The matrix elements of the v_{14} potential are displayed in fig. 11 for two particular values of k. Comparison between figs. 10 and 11 reveals a strong contrast between the behaviour of the two potentials. The matrix elements of v_{14} are dying off much more quickly than those of the Paris potential. Despite this strongly different behaviour, the two potentials yield the same phase shifts, i.e. the same on-shell

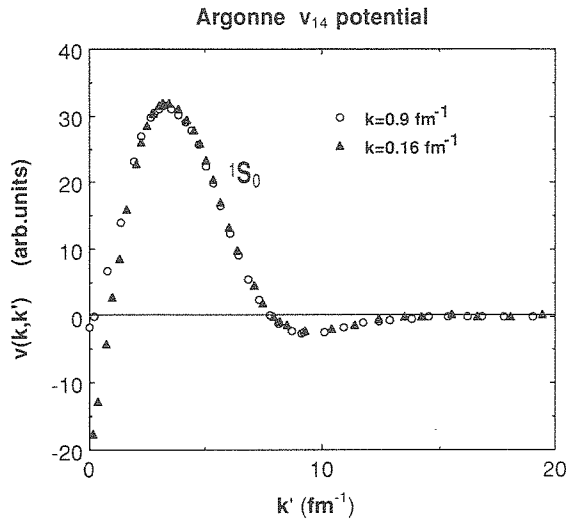

Fig. 11. Matrix elements $v(k, k')$ for the Argonne v_{14} potential.

T-matrix. Furthermore, as analyzed in ref. [41]), the off-shell behaviour of the T-matrix is not drastically different, if one restricts to deviations (in momentum as well as in energy) within about 1–2 fm^{-1} from the on-shell point.

4.4. ANALYSIS OF THE GAP FUNCTION

The considerations above enlightens our results. First the gap function Δ_k has the same asymptotic behaviour as the potential. In particular, it shows a node at $k \approx 6$ fm^{-1} which is precisely at the same place as in $v(k, k')$ for both Paris and v_{14} potentials. For the Paris potential, there is another node at a smaller k-value (~ 2 fm^{-1}) which comes from the almost coincident zeros in the form factors. The presence of the zero at practically the same place for the v_{14} potential is of less clear mathematical origin. In any case, the oscillations in the gap function Δ_k can be attributed physically to the presence of a hard core. Indeed, $\Delta(k)$ has the same nodes as $D(k)$ (eq. (3.1)). The Fourier transform $D(r)$ shows a "hole" at small relative distance ($r \lesssim 0.5$ fm) due to this core (see fig. 3b), similarly as the form factors. When Fourier-transformed back in momentum space, this generates an oscillation in $D(k)$ and, thence, in the gap function. The "hole" appears for the Paris and the v_{14} potential as well.

The gap equation may be considered as a Lippman–Schwinger equation when only a pole approximation at $E = 2\mu$ is retained (when the inhomogeneous term is dropped). Therefore it is expected that the gap function bears some resemblance with the half off-shell T-matrix at $E = 2\mu$. As we have seen, the properties of the latter are expected to be largely potential-independent in the $|k| \lesssim 2$ fm^{-1} range.

Therefore, the gap at the Fermi surface is expected to be the same for Paris and v_{14}. On the same grounds, one may expect a rather limited dependence for all realistic potentials. We note however that the difference between Paris and v_{14} should be attributed to the off-diagonal behaviour of these potentials. Furthermore, as the gap at $k \approx k_F$ is about the same for the two realistic potentials and since these potentials are quite different at large k' (for fixed k) they have also to be different at $k \approx k' \approx k_F$. This is in keeping with the behaviour of the Paris and v_{14} potentials as illustrated by figs. 10 and 11.

In conclusion, Δ_k at large k is governed by the off-diagonal behaviour of the potential. At small k and particularly at k_F, it is more or less independent of the potential and is expected to be roughly the same for all potentials reproducing correctly the low-energy phase shift. Its value is, however, not directly related to $v(k_F, k_F)$ and may involve large k-components of the interaction.

5. Analysis of the results

5.1. APPROXIMATION FOR THE GAP Δ_F

If in eq. (4.1), one makes the reasonable approximation $E(k') \approx \sqrt{(e(k')-\mu)^2+\Delta_F^2}$, the value of Δ_F can be obtained by imposing the full kernel $K(k, k')$ of the integral equation to have an eigenvalue equal to unity. If the kernel is discretized in $K_{ij} \approx K(k_i, k'_j)$, this condition is equivalent to

$$\det(\mathbf{1}-\mathbf{K}) = 0\,. \tag{5.1}$$

Another more transparent approximation can be obtained by assuming that $E(k')$ has the same value as above and furthermore that (i) the spectrum $e(k)$ corresponds to an effective mass (ii) the integration is effectively limited in an integral δk around k_F (iii) the interaction is constant in this interval. One then obtains (from (4.1))

$$\Delta_F \approx 4T_F^* \frac{\delta k}{k_F} \exp\left[4\pi^2 \frac{T_F^*}{v(k_F, k_F)k_F^3}\right], \tag{5.2}$$

with $T_F^* = \hbar^2 k_F^2/2m^*$. This approximation shows the right functional dependence upon the important parameters, but contains an arbitrary (a priori unknown) quantity δk. In the literature, formulae are usually given with $\delta k = 0.5 k_F$.

Using eq. (4.7) with $\Delta_{k'}$ proportional to $v(k', k_F)$ in the last term, one obtains

$$\Delta_F = 8T_F^* \exp\left[4\pi^2 \frac{T_F^*}{k_F^3 v(k_F, k_F)}\alpha\right], \tag{5.3a}$$

with

$$\alpha = 1 + \frac{1}{4\pi^2}\frac{2m^*}{\hbar^2}\frac{k_F}{v(k_F, k_F)}\int_0^\infty dx \frac{x^2 v(k_F, k_F x)^2 - (v(k_F, k_F))^2}{|1-x^2|}. \tag{5.3b}$$

Neglecting the integral in (5.3b) gives approximation (5.2) with, this time, $\delta k = 2k_F$. This apparent contradiction between these approximations can be removed if one isolates in the integral entering (5.3b) the contribution for k close to k_F. One finds

$$\Delta_F = \frac{2T_F^*}{\sqrt{1-(\delta k/4k_F)^2}} \exp\left[4\pi^2 \frac{T_F^*}{k_F^3 v(k_F, k_F)} \alpha_1\right], \tag{5.4a}$$

with

$$\alpha_1 = 1 + \frac{1}{4\pi^2}\frac{2m^*}{\hbar^2}\frac{k_F}{v(k_F, k_F)}\int_{1-\delta k/k_F}^{1+\delta k/k_F} \frac{x^2(v(k_F, k_F x))^2 - (v(k_F, k_F))^2}{|1-x^2|} + \left(\int_0^{1-\delta k/k_F} + \int_{1+\delta k/k_F}^{\infty}\right) \frac{x^2(v(k_F, k_F x))^2}{|1-x^2|}. \tag{5.4b}$$

The various approximations are compared in table 2 along with the exact value of Δ_F for a typical case. The "constant gap approximation" (eq. (5.1)) is particularly good. Approximation (5.2) looks more or less satisfactory in the middle of the superfluidity domain (large gap), but is quite bad at large k_F. Similarly the approximation of eqs. (5.3) and (5.4) is worse and worse as the Fermi momentum increases. Surprisingly, it is even worse compared to approximation (5.2), whilst it is expected to improve upon the latter by accounting for large-momentum effects by means of the last term in (5.4b). The latter introduces (at $k_F = 0.84\,\mathrm{fm}^{-1}$) a reduction of the gap by a factor 0.7 (for $\delta k = 0.5 k_F$). The deficiencies of approximation (5.3) come either from neglecting higher-order terms in eqs. (4.6) and (4.7) or from a crude treatment of the $k \approx k_F$ contribution (2nd term in eq. (5.4b)), especially for potentials like the Paris potentials, which are characterized by a large variation of $v(k_F, k')$ for $k' \approx k_F$ and for the values of k_F under investigation. In our opinion, the second possibility is the most likely.

There is also a popular approximation [42]) for the (Fermi momentum) gap $\Delta(T)$ at finite temperature T, which may be written as

$$\Delta(T) \approx \Delta(0)\left[1 - \sqrt{\frac{2\pi T}{\Delta(0)}}\, e^{-\Delta(0)/T}\right], \tag{5.5}$$

TABLE 2

Comparison between the exact value of the gap Δ_F in neutron matter and various approximations (in MeV). See text for detail

k_F (fm^{-1})	Δ_F (exact)	Δ_F (approx. (5.1))	Δ_F (approx. (5.2))	Δ_F (eq. (5.3))
0.6	2.28	2.31	2.05	4.20
0.84	2.73	2.70	4.23	6.21
1.1	1.83	1.90	5.38	7.08

for $T \ll \Delta(0)$ and

$$\Delta(T) \approx \left[\frac{8\pi^2 T^2}{7\zeta(3)} \frac{1}{\ln[\gamma\Delta(0)/\pi T]}\right]^{1/2} \tag{5.6}$$

for $T \gg \Delta$, where ζ is the Riemann function and γ the Euler constant. The approximate value of the transition temperature is then given by

$$T_c = \frac{\gamma\Delta(0)}{\pi} = 0.57\Delta(0)\,. \tag{5.7}$$

Our calculated values do not deviate significantly from this approximation, an observation which is also made in refs. [15,21]).

5.2. IMPLICATIONS OF OUR RESULTS

As for neutron matter, our results corroborate previous results and point to the fact that the neutron gas penetrating the nuclei lattice in the inner crust of neutron stars should be superfluid. There is only limited quantitative difference with previous estimates as far as the value of the gap and the phase diagram are concerned.

We also presented the gap function Δ_k up to large values of k. Especially for the Paris potential, this gap function fluctuates of sign and dies off at large k-values only. As a consequence, the pairing function $D(k)$ is asymmetric. Therefore, it is expected that the weak-coupling formula for the condensation energy per particle

$$\frac{E_C}{A} = \frac{3}{8}\frac{\Delta^2}{T_F^*} \tag{5.8}$$

is not very accurate in our case. This is illustrated by table 1, at least for one potential. Except in the region around the maximum value of the gap, where eq. (5.8) introduces only a 1–2% error, it is rather bad for the remaining range.

For nuclear matter, our calculation shows that the gap does not vanish at saturation density ($k_F = 1.35\ \mathrm{fm}^{-1}$), although it has a small value ($\Delta_F \approx 0.3$ MeV). This value is intermediate between the ones obtained in ref. [21]) for Reid and Bethe–Johnson potentials and the one given in ref. [23]) for the effective Gogny potential. In nuclei, the condensation (pairing) energy would then come mainly from the nuclear surface.

6. Comparison with other works

As far as realistic potentials are used and the gap equation is fully solved, our work can be compared with that of refs. [13–21]), although the schemes may be quite different (semi-realistic interactions, g-matrix or equivalent interactions, inclusion of higher-order terms, ...). In this section, we limit ourselves to a discussion of the works disregarding the second-order (polarization) interaction. The latter is briefly discussed in the next section.

Surprisingly enough, there are very few calculations using bare realistic interactions. The work of ref. [16]) is one example, although the interaction used consists of a one-pion exchange part supplemented by a gaussian soft core (OPEG) and cannot really rival with the Paris potential for fitting two-nucleon data. Also, as we did, Takatsuka [16]) introduces the Brueckner single-particle energies. The comparison is given in fig. 12a. There is a rather small difference between our calculation for the Paris (and also v_{14}) potential and the similar calculation of ref. [16]) for the OPEG potential. The calculation of ref. [17]), also shown in fig. 12a, deals with the same OPEG potential but uses single-particle energies which are obtained in the Hartree approximation. This amounts to modifying the effective mass, but also the chemical potential. Due to the structure of the gap equation [eqs. (2.2) and (2.3)], the modification of the latter emphasizes a slightly modified momentum range.

In fig. 12b, we compare results for the gap obtained with renormalized interactions, all obtained in the context of correlated wave functions, either in the simple variational (Jastrow-like) approach or in the hypernetted-chain approach. For OPEG potential one has a direct comparison between a calculation with the bare interaction and a calculation with the variational effective interaction, keeping the single-particle spectrum unchanged (except possibly for slight changes, due to the self-consistent determination of the occupation probabilities entering in the Hartree approximation). It can be seen from fig. 12a, b that the introduction of the effective interaction

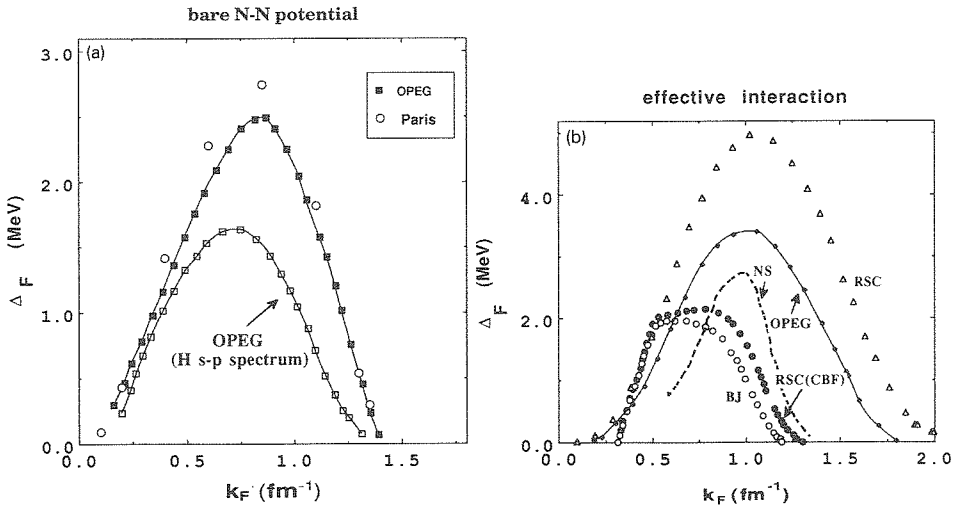

Fig. 12. Comparison between various works concerning neutron matter superfluidity. (a) For bare interaction: Paris potential (open dots), our work, OPEG potential with Brueckner-Hartree-Fock single-particle spectrum (black squares), ref. [16]); same potential with Hartree spectrum (open squares), ref. [17]). (b) For effective interaction: Reid soft-core potential (triangles), ref. [17]), Reid soft core (full dots), ref. [21]), Bethe-Johnston (open dots), ref. [21]) and OPEG (full line), ref. [17]). The dotted line represents the results obtained in second order by Niskanen and Sauls (ref. [20])), as quoted in ref. [17]). See text for detail.

enhances the maximum gap value and broadens the superfluidity domain (in k_F). This likely results from the fact that Jastrow correlations cut the short-range (repulsive) part of original interaction in building the effective one. However, the two calculations mentioned RSC in fig. 12b have been obtained with the same Reid soft-core interaction. One (indicated by triangles) is done with the effective interaction in the simple Jastrow scheme with Hartree-like single-particle energies, and the other uses a more refined (hypernetted) scheme, including for the single-particle spectrum. According to ref. [18]), this should only introduce minor changes. The strong differences may be attributed (in the opinion of the authors of ref. [21])) to the "omission of the correlation kinetic energy portion of the effective interaction" by the authors of ref. [17]), which leads to an overestimation of the gap. Unfortunately, the size of this effect is not quantitatively known. Therefore, without resorting to the appropriateness of using effective interactions, one can in the actual situation not determine very precisely in which proportion the gap is changed, in comparison with a calculation using bare interactions. To say the least, even in the lowest order, the situation is rather obscure and our work appears (at this order) as one of the rare well-defined and precise calculations. It should be noticed however that within a particular scheme realistic interactions yield very similar results. This is corroborated by our results (fig. 1) and also by the results of ref. [21]) (open and full dots of fig. 12b).

If the calculations cited above differ on the maximum value of the gap in neutron matter, they also disagree on the domain of superfluidity (in k_F). Except for the calculations of ref. [17]), using effective interactions, most of them predict a closing of the domain between ~ 1.3 to $\sim 1.5\ \mathrm{fm}^{-1}$. Surprisingly, there are also differences for the lower limit of the domain. In particular, the authors of ref. [21]) (see fig. 12b) predict this limit to lie around $\sim 0.25\ \mathrm{fm}^{-1}$ whereas, for all the other ones, it falls below $0.1\ \mathrm{fm}^{-1}$.

The gap function Δ_k is also given in ref. [17]). If one compares fig. 3 of this reference and our fig. 2, one can see that the shape of this function is largely independent of the force. However, as underlined in sect. 4, the overall decrease of Δ_k is slower for the Paris potential compared to other potentials and can be traced back to its short-range behaviour.

7. Discussion and conclusion

We solved here the gap equation for two realistic potentials, using the bare potential (and accessorily the g-matrix) and a single-particle spectrum calculated in the Brueckner–Hartree–Fock approximation. This procedure has been suggested by Cooper, Mills and Sessler [3]) and is closely related to the method, advocated by Emery [43,44]), which identifies the existence of a singularity in the Bethe–Goldstone equation as the signal for superfluidity. Furthermore, the Green function approach to superfluidity leads to a gap equation where the single-particle spectrum should

contain ordinary (mainly short-range, in neutron and nuclear matter) correlation effects and where the pairing interaction contains all possible irreducible particle–particle diagrams. The simplest ones are given in fig. 13. The first term is then the bare interaction.

Disregarding the results of the Green function, the superfluidity problem has been attacked by using variational methods, generalizing in some sense the original BCS theory. In particular, this has been done in the frame of the Jastrow and correlated wave functions. One then minimizes the free energy in the subspace of wave functions (2.1) multiplied by some Jastrow-like correlation terms. A gap equation is obtained with, in lowest order, a pairing interaction which roughly corresponds to the bare interaction multiplied by the square of the correlation function, very much resembling the Brueckner g-matrix. Note, however, that the variational problem defined this way is not strictly a Ritz variational principle.

Coming back to the pairing interaction as defined by fig. 13, the first correction term (called the polarization graph) has been studied in some detail in refs. [20,21]), which arrive at different conclusions. It seems [20]) however, that density fluctuations (i.e. the central part of the interaction exchanged in the second graph of fig. 13) enhance the gap whereas the spin fluctuations [21]) reduce it. The prediction of ref. [20]) is shown by the dotted line of fig. 12b. It should be compared to the full dots of fig. 12b, which corresponds to a calculation with the same interaction neglecting polarization effects. In ref. [21]), the first-order pairing interaction is corrected for higher-order terms, including the polarization graph, leading to a large reduction of the gap (factor ~4). However, the correction includes, besides the polarization graph, several other corrections typical to the correlated basis formalism and it is therefore hard to assess the contribution of the polarization alone. Furthermore, in ref. [21]), infinite number of loops are introduced through the Landau parametrization of the residual interaction, whereas the calculation of ref. [21]) is limited to the one loop approximation. Therefore, it can be concluded that the effect of the polarization graph is not quantitatively well known. The issue is thus still open and deserves further investigation.

As for the astrophysical applications, our results, even when corrected for polarization, would have minor effects. The inner-crust neutrons do not participate significantly to the cooling of neutron stars. However, their superfluid properties may be more important for the description of the neutron star rotation speed-up in so-called glitch phenomena [18,45]). On the other hand, the $^1S_0$ proton superfluidity

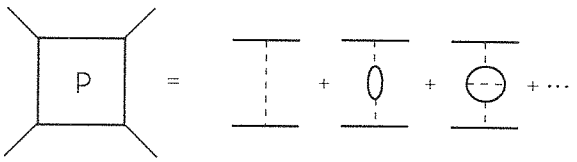

Fig. 13. Schematic representation of the pairing interaction, following ref. [30]).

for the proton component in the neutron background around saturation nuclear matter density and the $^3P_2{}^3F_2$ superfluidity play a crucial role in the cooling of neutron stars. These problems are, however, more complicated than $^1S_0$ neutron pairing and they will be tackled in a forthcoming publication. In the first case, one has to take account of the neutron background influence on the proton-proton pairing interaction. In the second, one has to work out properly the self-consistency treatment in the anisotropic gap equations.

For nuclear matter, our calculations seem to indicate that the Paris potential (and also v_{14}) gives a too small condensation energy in nuclei (the value of the latter seems to be fixed by systematical study of binding energy, fission barriers [46]) and Hartree-Fock-Bogoliubov calculations [39])). This seems to be linked to a closing of the superfluid domain at too small density. However, the superfluid properties of nuclear matter can be due to interactions in other channels than the $^1S_0$. Recently [47]), it has been suggested that nuclear matter at ordinary density could be a very strong $^3S_1{}^3D_1$ superfluid.

We would like to thank Drs. W. Dickhoff and P. Schuck for helpful discussions.

References

1) A. Bohr, B. Mottelson and D. Pines, Phys. Rev. **110** (1958) 936
2) J. Bardeen, L.N. Cooper and J.R. Schrieffer, Phys. Rev. **108** (1957) 1175
3) L.N. Cooper, R.L. Mills and A.M. Sessler, Phys. Rev. **114** (1959) 1377
4) V.J. Emery and A.M. Sessler, Phys. Rev. **119** (1960) 248
5) J.M. Lattimer and D.G. Ravenhall, Astrophys. J. **223** (1978) 314
6) A.B. Migdal, Sov. Phys. JETP **10** (1960) 176
7) D. Pines, J. de Phys. **41** C2 (1980) 111
8) V.L. Ginzburg, J. Stat. Phys. **1** (1969) 3
9) G. Baym, C. Pethick, D. Pines and M.A. Ruderman, Nature **224** (1969) 872
10) J.W. Clark and N.C. Chao, Lett. Nuovo Cim. **2** (1969) 185
11) J.W. Clark, Phys. Rev. Lett. **23** (1969) 1463
12) E. Østgaard, Nucl. Phys. **A154** (1970) 202
13) E. Østgaard, Z. Phys. **243** (1971) 79
14) C.H. Yang and J.W. Clark, Nucl. Phys. **A174** (1971) 49
15) N.C. Chao, J.W. Clark and C.H. Yang, Nucl. Phys. **179** (1972) 320
16) T. Takatsuka, Prog. Theor. Phys. **48** (1972) 1517
17) L. Amundsen and E. Østgaard, Nucl. Phys. **A437** (1985) 487
18) E. Krotscheck and J.W. Clark, Nucl. Phys. **A333** (1980) 77
19) J.W. Clark, C.-G. Källman, C.-H. Yang and D.A. Chakkalakal, Phys. Lett. **B61** (1976) 331
20) J.A. Niskanen and J.A. Sauls, 1981, unpublished
21) J.M.C. Chen, J.W. Clark, E. Krotscheck and R.A. Smith, Nucl. Phys. **A451** (1986) 509
22) M.F. Siang and T.T.S. Kuo, Nucl. Phys. **A481** (1988) 294
23) H. Kucharek, P. Ring and P. Schuck, Z. Phys. **A334** (1989) 119
24) J. Dechargé and D. Gogny, Phys. Rev. **C21** (1980) 1568
25) W.H. Dickhoff, Phys. Lett. **B210** (1988) 15
26) M. Lacombe, B. Loiseaux, J.-M. Richard, R. Vinh Mau, J. Côté, D. Pirès and R. de Tourreil, Phys. Rev. **C21** (1980) 861
27) P. Grangé, M. Martzolff, J.-F. Mathiot and A. Lejeune, Phys. Rev. **C40** (1989) 1040

28) P. Grangé, J. Cugnon and A. Lejeune, Nucl. Phys. **A473** (1987) 365
29) I.E. Lagaris and V.R. Pandharipande, Nucl. Phys. **A359** (1981) 331
30) A.B. Migdal, Theory of finite Fermi systems and applications to atomic nuclei (Wiley, New York, 1967)
31) P. Nozières, Theory of interacting Fermi systems (Benjamin, New York, 1964)
32) P. Ring and P. Schuck, The nuclear many-body problem (Springer, Berlin, 1980)
33) P.W. Anderson and P. Morel, Phy. Rev. **C123** (1961) 1911
34) J. Haidenbauer and W. Plessas, Phys. Rev. **C30** (1984) 1822
35) A. Lejeune, P. Grangé, M. Martzolff and J. Cugnon, Nucl. Phys. **A453** (1986) 189
36) M. Baldo, I. Bombaci, L.S. Ferreira, G. Giansiracusa and U. Lombardo, Phys. Lett. **B215** (1988) 19
37) M. Baldo, L.S. Ferreira, T. Vertze and L. Streit, Phys. Rev. **C33** (1986) 1587
38) D.J. Ernst, C.M. Shakin and R.M. Thaler, Phys. Rev. **C8** (1973) 507
39) H. Kucharek, P. Ring, P. Schuck, R. Bentsson and M. Girod, Phys. Lett. **B216** (1989) 249
40) F.G. Tricomi, Integral equations (Wiley, New York, 1957)
41) E.F. Redish and K. Stricker-Bauer, Phys. Rev. **C36** (1987) 5130
42) E.M. Lifshitz and L.P. Pitaevskii, Statistical physics (Pergamon, Oxford, 1980) p. 159
43) V.J. Emery, Nucl. Phys **12** (1959) 69
44) V.J. Emery, Nucl. Phys. **19** (1960) 154
45) D. Pines and M.A. Alpar, Nature **316** (1985) 27
46) M. Beiner, H. Flocard, Nguyen Van Giai and Ph. Quentin, Nucl. Phys. **A328** (1975) 29
47) W.H. Dickhoff *et al.*, Proc. of recent progress in many-body theories, ed. Y. Avishai *et al.* (Plenum, New York) to be published